

Integration of Large Wind Farms into Utility Grids (Part 1 - Modeling of DFIG)

Rodolfo J. Koessler, *Senior Member, IEEE*, Srinivas Pillutla, *Member, IEEE*, Lan H. Trinh, *Member, IEEE*, and David L. Dickmader, *Member, IEEE*
ABB Inc.

Abstract—In this part of the paper the authors describe a newly developed model for doubly-fed induction wind generators (DFIG) that is suitable for transient stability studies. In this model the main performance characteristics of DFIG are included. The model is validated against a more detailed EMTP-level model of such generation. The results suggest that the stability model has sufficient accuracy for representation of the electromechanical dynamics of interest in simulation studies for identifying critical operating conditions. Further analysis of these critical conditions may require the use of more detailed EMTP-level models.

Index Terms— Wind turbine generators, wind energy, modeling wind farms.

I. INTRODUCTION

The last few years have seen the emergence of wind generation as the leading source of renewable energy in the power industry. Wind farms totaling hundreds, even thousands, of MW are now being considered. “Making room” for this new type of generation in electric networks poses significant challenges on a wide range of issues. This paper addresses one of those issues, namely the modeling of doubly-fed induction generators (DFIG) for a more accurate and realistic assessment of the transient stability performance of the system. DFIG is one of the two main types of wind generation currently in use (the other is conventional induction generators) and its performance aspects are just starting to be addressed in the technical literature. One important step in assessing such performance is the development of a suitable dynamic model of DFIG for use in “transient stability” programs. This paper discusses the derivation and validation of one such model. The validation steps included the verification of:

- steady-state initialization
- small-signal performance
- performance following large disturbances

As opposed to the equivalencing approach usually utilized in the technical literature, the model described in this paper explicitly simulates some of the main aspects of DFIG, such as slip-frequency rotor dynamics, and current controls. The general principles described here are applicable to any stability program. We coded and tested a user-defined model for DFIG on a widely-used commercial program for power system simulations (PSS/E). Also described in this paper is a detailed “EMTP-type” three-phase model of DFIG developed in the Matlab program, against which the stability model was validated.

II. GENERAL DESCRIPTION OF DFIG

The principles of DFIG have been discussed in a variety of papers, and thus are only summarized here. A DFIG is essentially a wound rotor induction generator with slip rings. DFIG differs from synchronous generation in that the rotor is fed from a three-phase variable-frequency source, thus allowing DFIG units to operate at a variety of speeds. This ability to vary operating speed is important in wind generation because it allows for an optimization of the transfer of power from the wind to the turbine blades.

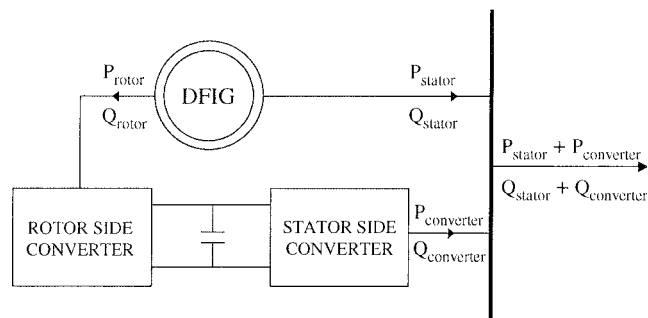


Fig. 1. Schematic of DFIG-type Wind Generation.

The variable-frequency supply to the DFIG rotor is attained via the use of two voltage-source converters linked via a capacitor (See Fig. 1). The rotor-side converter feeds the DFIG rotor with the active and reactive power necessary to attain its control objectives; usually consisting of maintaining turbine speed, and, in some cases, either controlling stator-side power factor, and/or terminal voltage. Active power

requirements for this rotor-side converter are provided by drawing current from or supplying current to the capacitor linking the rotor- and stator-side converters. The main objective of the stator-side converter is to maintain control of the voltage level on the dc bus capacitor by exchanging active power with the grid. In so doing, the stator-side converter is essentially transferring to the terminals of the machine the active power requirements of the rotor. The stator-side converter also has the ability to control terminal voltages and/or power factor by exchanging reactive power with the grid, doubling as an SVC or STATCOM function.

Because rotor- and stator-side converters handle ac quantities (of slip and grid frequency, respectively), they are controlled utilizing vector-control techniques. In a nutshell, vector control is based on the concept of developing a rotating reference frame based on an ac flux or voltage, and projecting currents on such a rotating frame. Such projections are usually referred to as the d and q components of their respective currents. With a suitable choice of reference frames, the ac currents appear as dc quantities in the steady-state. For flux-based rotating frames, changes in the d component will lead to reactive power changes; changes in the q component of current will vary active power exchanges. In voltage-based rotating frames (and thus 90 deg. ahead of flux-based frames) the effect is the opposite. The d and q components are normally driven to reference levels via only proportional (P) controllers, or both proportional + integral (PI) controllers. In DFIG the reference levels are in turn typically set by controllers such as:

- An electrical torque controller driving the rotor-side converter i_q controller (flux-based controller).
- Capacitor voltage controller driving the stator-side converter i_d controller (voltage-based controller).
- Power factor and/or ac voltage controllers driving the i_d and i_q controllers on either (or both) rotor- and stator-side converters, respectively.

A typical implementation of such control concepts is detailed in [1]. The controller models in this paper followed the general principles described in that reference, with adjustments necessary to make them applicable to the typical DFIG generator parameters assumed in these studies.

III. DETAILED DFIG MODEL

As previously indicated, the transient stability model of the DFIG was benchmarked against the corresponding EMTP-level model. This latter three-phase model (written in the Matlab language), including representation of stator flux derivatives, followed for the most part the control structure described in [1]. The model also includes representation of typical filtering and transducer dynamics. Additionally, the following limitations were represented:

- Non-windup limit on i_d order in stator-side converter (capacitor voltage control).

- Windup limit on voltage order in rotor-side converter.
- Non-windup limit on i_q order in rotor-side converter (speed control).

To reduce computation time requirements, the detailed model neglects high frequency effects of the PWM firing scheme, and instead models the output of the voltage source converters as the average over each PWM cycle.

A 60 Hz, 1750 kW, 0.9 pf, 600 V (stator), 1800 V (rotor) transient-level wind generator was modeled, with parameters as listed in Table I. Generator saturation was not modeled. A rated slip of -20% was assumed (i.e., a rotor speed of 72 Hz). DFIG generators are usually rated at super-synchronous speeds since, as will be shown in Section IV, at those speeds power flows out of both stator and rotor, and thus maximum use is made of the generator capabilities.

TABLE I
DFIG MODEL PARAMETERS

X (pu)	X' (pu)	Xl (pu)	Rs (pu)	T' (sec)	H (pu)
3.00	0.300	0.150	0.005	1.5	3.00

The above set of nameplate data and dynamic model parameters were assumed on both the detailed and on the transient stability model; thus allowing the independent confirmation of results from the latter model. This validation process is described in Section IV.

As in other areas of power system analyses, the advantage of EMTP-level models is in their modeling detail; their disadvantage is that simulations of large systems with such modeling detail are usually not practical. Thus, the use of EMTP is normally reserved to situations where such level of detail is required. As will be seen later, EMTP-level simulations, in combination with transient-stability studies, are likely to play an important role in studies involving DFIG.

IV. DEVELOPMENT AND VALIDATION OF THE TRANSIENT STABILITY MODEL

A. Modeling of the Generator

A slight variation of a fourth order subtransient-level model with saturation, normally utilized to represent round-rotor synchronous generators (the GENROU model in the PSS/E program [3]), was utilized to simulate the generator part of the DFIG. Whereas the synchronous machine model assumes excitation (E_{fd}) on the direct axis only, in the DFIG model the code was modified so as to allow for quadrature axis excitation (E_{fq}) too. The other significant difference between the models is that, whereas the synchronous machine model is normally initialized at synchronous speed, and thus with constant d and q axis magnitudes, the DFIG model is designed to be initialized at a user-defined slip frequency. Thus, provisions had to be made for initializing fluxes and currents as slip-frequency sinusoidal magnitudes. Due to the

symmetry of the rotor, this was done by representing generator variables as slip-frequency phasors, thus establishing states, state derivatives, field voltages and currents as complex magnitudes, and projecting them onto an arbitrarily-selected dq reference frame fixed on the rotor for initialization of the d and q parameters in the model. Provision was also made to make sure that the integration algorithm correctly recognized the non-zero initial state derivatives, and thus that the first time step was being correctly integrated.

B. Steady-State Validation of Generator Model

For the purposes of validating the initialization process, the EMTP-type and transient stability models were initialized at the assumed rated conditions. Inputs to the generator initialization process are the stator terminal conditions (as defined in the loadflow) and the assumed speed. The assumed operating point is summarized in Table II and was equally applied to both models. The results from the initialization process are the rotor terminal magnitudes, as well as the required turbine mechanical power (or torque). These results from each of the models are summarized in Table III and suggest an adequate correlation between the two models. At these assumed super-synchronous conditions, power from the turbine is channeled through both the stator and rotor, for a total output of about 1,731 kW.

TABLE II

INPUT TO THE INITIALIZATION PROCESS (FROM LOADFLOW + USER INPUT)

Pstator (kW)	Qstator (kVar)	Vstator (V) (l-g)	Speed
1,448	258	353	72 Hz.

Having validated the initialization algorithm, some interesting observations on the steady-state behavior of DFIG were obtained. For example, initialization of the generator at 120%, 100% and 80% of synchronous speed while maintaining the stator conditions in Table II resulted in the rotor terminal magnitudes listed in Table IV.

TABLE III

RESULTS FROM THE INITIALIZATION PROCESS

Model	Protor (kW-Out)	Qrotor (kVar-Out)	Vrotor (V) (l-g)	Torque (pu 1944 kVA)
Detailed	283	286	236	0.750
Stability	282	285	234	0.748

Active power flowing into the rotor is comprised of the following two components:

- Rotor Losses
- Slip*(P_{stator}+Stator Losses)

Thus, when the DFIG operates at super-synchronous speeds, power flows out of both stator and rotor, whereas, when operating at sub-synchronous speeds, power is still generated at the stator, but is consumed at the rotor. As in the case of synchronous generators, during synchronous operation the rotor-side converter furnishes the rotor losses only. The

results in Table IV confirm that, whereas in synchronous machines the ratings of excitation systems are small compared to those of the generator, that is not the case for the converter ratings in DFIG units.

Also interesting to observe in Table IV is the fact that, whereas in a synchronous generator the quantity E_{fd} (equal to $e_{fd} * L_{ad} / r_f$) will typically range between 2 and 4 per unit, in DFIG the magnitude of rotor voltage can be many times higher. This is because, in the steady-state:

$$E_f = \frac{\partial \psi_f}{\partial t} * L_a + L_a * I_f \quad (1)$$

where $E_f = E_{fd} + j E_{fq}$, Ψ_f and I_f represent the per-unit magnitudes of the rotor flux linkages and rotor current, respectively. L_a and r_f represent the per-unit stator-to rotor mutual inductance and the field resistance, respectively.

For operation at super- and sub-synchronous speeds, the first term in Equation (1) will normally be the dominant component. In the above exercise, for example, the magnitude of the first term when operating at 72 Hz is 122.62 pu, whereas that of the second factor is 2.61 pu; not coincidentally, the same as in the synchronous speed case in Table IV. The quantity E_f should not be confused with per-unit rotor voltage e_f . For synchronous generators, e_f is in the order of 0.01 pu. For the DFIG at 72 Hz example shown in Table IV, an E_f of 120.77 pu is equivalent to an e_f of 0.225 pu, which appears large for a synchronous generator, but is quite reasonable for DFIG.

TABLE IV

INITIALIZATION AT DIFFERENT SPEEDS

Speed (Hz)	Protor (kW - Out)	Qrotor (kVar - Out)	Mag(Ef) (pu)
72	282	285	120.77
60	-8.66	0	2.61
48	-299	-285	124.49

C. Development of DFIG Control Models

Having developed and validated the generator model itself, models of the DFIG controls were developed next. The following control loops for the rotor-side converter were explicitly modeled:

1. i_q PI Controller
2. i_d PI Controller
3. Speed PI Controller driving the i_q Control reference
4. Voltage Controller driving the i_d Control reference.

Loops 1 through 3 were modeled as described in [1]. The control of terminal voltage was modeled with a gain and time constant, much in the same way that an SVC can be controlled [2]. The following limitations were also modeled:

- Non-windup limits on the i_d and i_q orders; outputs of Loops 3 and 4 above.
- Windup limit on converter voltage order.

With regards to the modeling of controls for the stator-side converter, for simplification purposes, the DFIG model was coordinated with the PSS/E Model CBES; which is a simplified model of a Battery Energy Storage system [3]. The CBES model contains two paths; one processing an active power order, the other modeling a voltage controller driving the reactive power control. The DFIG and CBES models were coordinated by making the CBES active power order equal to the DFIG rotor power. Further, the CBES model was instructed to limit its grid-side current, thus emulating current order limitations constraining the capacitor voltage controller in the stator-side converter. Thus, as will be seen later, any discrepancy between active power order from the DFIG model, and actual power output from the CBES (stator-side converter) model is indicative of a scenario of potential overcharging or undercharging of (and, thus, voltage excursions on) the capacitor linking the two converters.

D. Small-Signal Validation of DFIG Model

The small-signal performance of the rotor-side converter current and speed controls was assessed by applying a step-change on their respective integrator states, and then letting the loops "ring down" to their pre-disturbance levels. Shown in Fig. 2 are the resulting responses of the current control PI outputs for the detailed and stability models. Fig. 3 illustrates equivalent responses for the speed control PI Outputs.

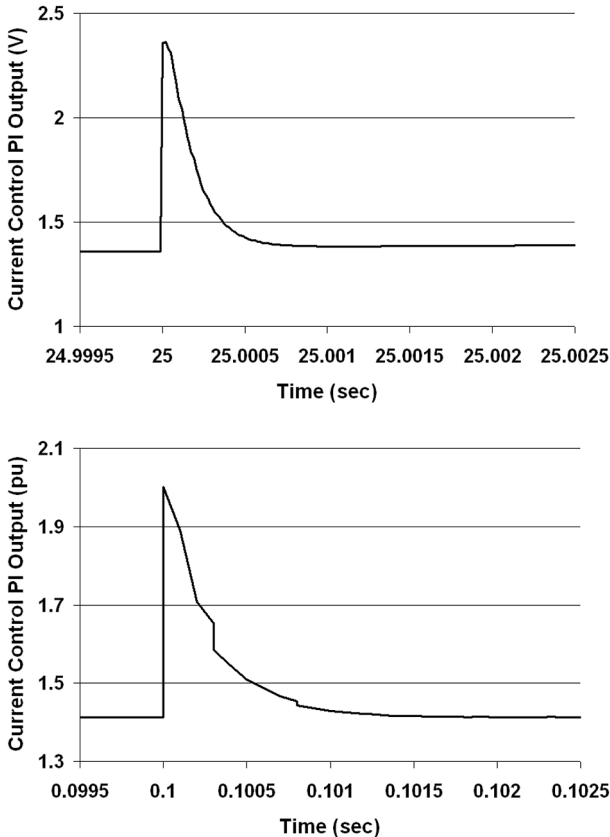


Fig. 2. Step on Current Control Integrator States. PI Control Outputs. Detailed vs. Stability Models.

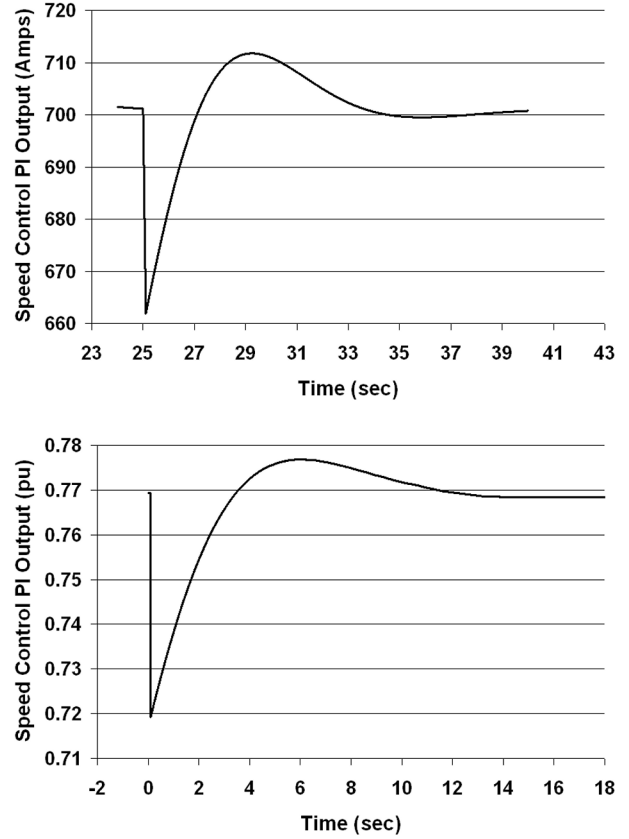


Fig. 3. Step on Speed Control Integrator States. Detailed vs. Stability Models.

The results suggest a good agreement between the two models, both in the shape and the speed of their responses to the disturbance. The speed of the response is determined by the proportional gain of the control. In the case of the current control, such speed can be calculated as:

$$W_c (\text{Current Loop}) = \frac{K_p * 2 * \pi * 60}{\sigma * (L_f + L_a)} * \frac{r_f}{L_a} = 3,721 \text{ rad/sec} \quad (2)$$

with σ as defined in [1]:

$$\sigma = 1 - \frac{L_a^2}{L * (L_f + L_a)} \quad (3)$$

In the above equations, r_f and L_f represent the per-unit resistance and leakage inductance of the field circuit, respectively. L is the per-unit stator inductance. K_p is the proportional gain of the controller.

That is, the speed of the current control loop is approximately $1/60^{\text{th}}$ of a 60 Hz cycle.

The speed control loop, on the other hand, is significantly slower:

$$W_c (\text{Speed Loop}) = \frac{K_p * L_a * \lambda_{ds}}{2 * H * L} = 0.309 \text{ rad/sec} \quad (4)$$

with λ_{ds} the magnitude of the stator-flux oriented reference frame, as defined in [1].

Finally, and for illustration purposes, shown in Fig. 4 is the detailed (EMTP-level) model's response to a perturbation in the stator-side converter dc voltage control loop. This loop was assumed instantaneous in the DFIG/CBES model. Comparing Fig. 4 against the current loop test results in Fig. 2, suggests that the voltage control is approximately 10 times slower than the current controls (which is expected, since the voltage control drives the i_d controller in the stator-side converter).

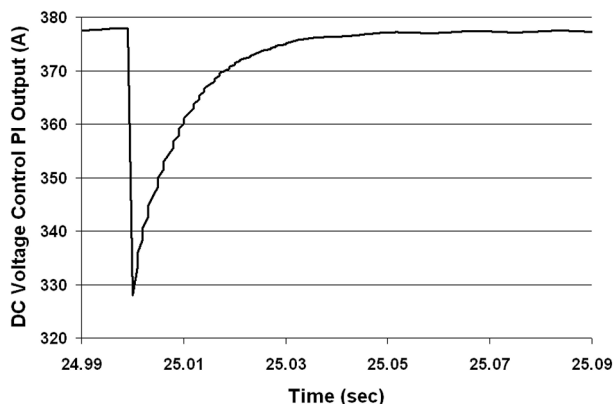


Fig. 4. Step on dc Voltage Control Integrator State. Detailed Model.

These results suggest a good match between detailed and stability model for small disturbances. They also show that the dynamics of current controllers in DFIG are much faster than the electromechanical dynamics of interest in transient stability simulations. Simulating fast processes such as these requires the use of a small time step for numerically integrating the system differential equations. This could potentially slow down system studies to the point of rendering them impractical for large power systems. In some instances, however, such dynamics might be of interest to the analyst, such as when assessing DFIG performance during a fault. In order to resolve this dilemma, the model was furnished with the ability to perform internal integration between steps used in the stability program. Further, the number of internal integration steps was made user-selectable, thus allowing the analyst to choose an appropriate combination of "internal" and "external" time step size (including making them equal) that better fits the user.

E. Large-Signal Validation of DFIG Model

The stability model was validated by subjecting it to disturbances of different severities and comparing results against those of the detailed model. In this section simulation results are presented for one of the most severe scenarios studied; a 4-cycle 1 milliohm fault at the generator terminals.

Shown in Fig. 5 are rotor currents during the fault as calculated by the detailed and stability models. As stator currents surge upon fault inception, so do rotor currents. The aggressive setting of current controllers, however, manages to quickly restore rotor (and stator) currents to pre-contingency levels; even while the fault is still being applied. The stability model manages to capture a significant portion of these phenomena.

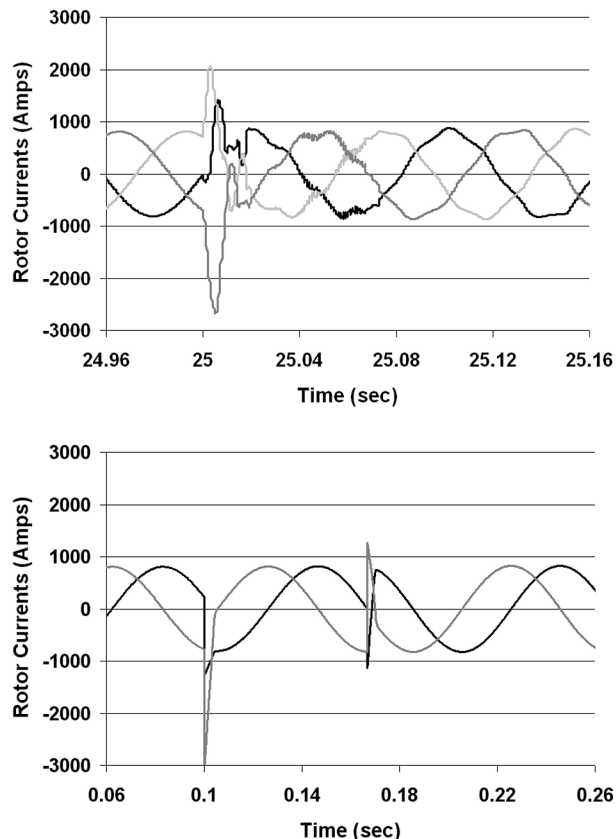


Fig. 5. 4-cycle 1 mOhm Fault at Generator Terminals – Rotor Currents - Detailed vs. Stability Models (3-phase components for Detailed Model, dq components for Stability Model).

The agreement between the two models, however, is not as good when considering the rotor voltage traces in Fig. 6. This is because of three factors. First, the output of the rotor side converter is limited by the dc bus rail voltages during the fault, resulting in clipping of the ac waveform. Note from Fig. 6 that, as previously described, a PWM-averaged model of the converter bridge is used in the detailed model, and therefore the voltage shown in Figure 6 should be interpreted as the average value over each PWM cycle. During the fault, the rotor converter duty cycles are driven to the plus and minus dc rails, giving clipping of the fundamental component of the voltage waveform.

Second, the effect of the dc current components initiated by the fault is significant. The loss of volt-seconds during the fault results in dc currents in the machine stator after fault clearing. These dc currents result in 60 Hz perturbations in

all rotor-frame control quantities, and are also seen in the rotor side currents. The L/R time constant involved in the decay of the stator-side dc currents is relatively long for the system parameters used in the model.

Finally, due to the large gains of current controllers that attempt to hold currents constant, the above effects (that are, of course, not captured by the fundamental-frequency stability model) lead to a significant harmonic, and non-linear, content on the converter-driven rotor voltages; content that subsists for some duration even after the fault is cleared.

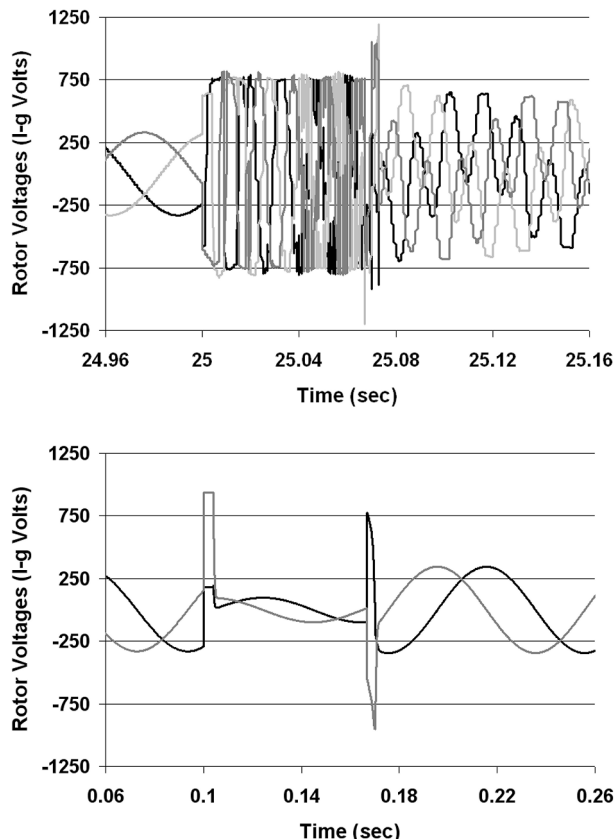


Fig. 6. 4-cycle 1 mohm Fault at Generator Terminals – Rotor Voltages - Detailed vs. Stability Models (3-phase components for Detailed Model, dq components for Stability Model).

Due to the integrating or smoothing effect of inertia, however, these non-linearities and harmonic content do not appear to significantly affect the electromechanical dynamics of the generators, as suggested by the relatively good agreement between the two speed traces (detailed vs. stability models) in Fig. 7. Good agreements were also observed following less severe faults.

The transient stability model cannot correctly compute potential overvoltages on the capacitor linking the two converters following large disturbances. As explained in Part 2 of this paper [4], immediately following a fault, there is “rush” of active power from the rotor terminals towards the converter, power that the converter redirects towards the

capacitor linking rotor- and stator-side converters. At the same time, due to low voltages at machine terminals, the stator-side converter is limited in its ability to “carry through” this extra power to the grid. Consequently, charging (and thus voltage) on the capacitor rises, which could lead to the bypassing of the capacitor (via a crowbar) in order to preserve the integrity of the converters. This, in turn, would lead to the tripping of the unit.

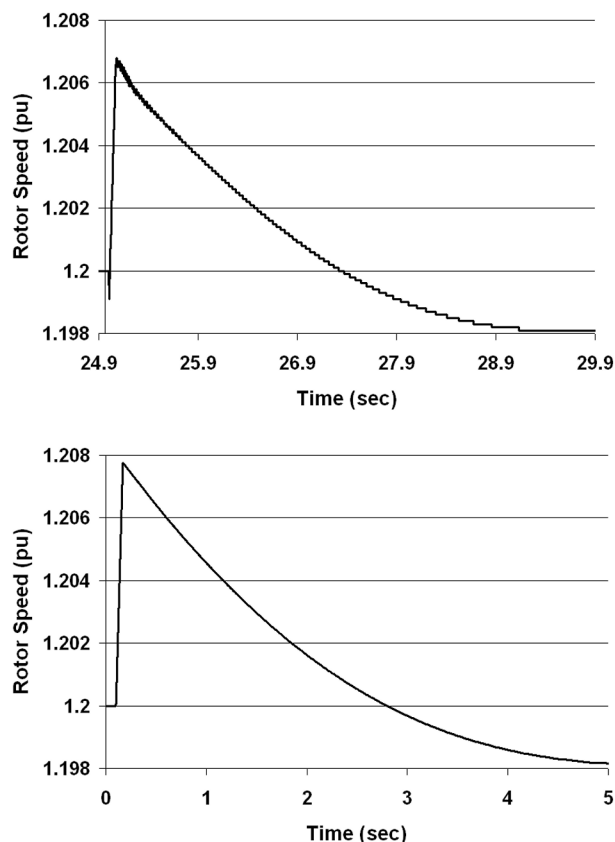


Fig. 7. 4-cycle 1 mohm Fault at Generator Terminals – Unit Speed - Detailed vs. Stability Models.

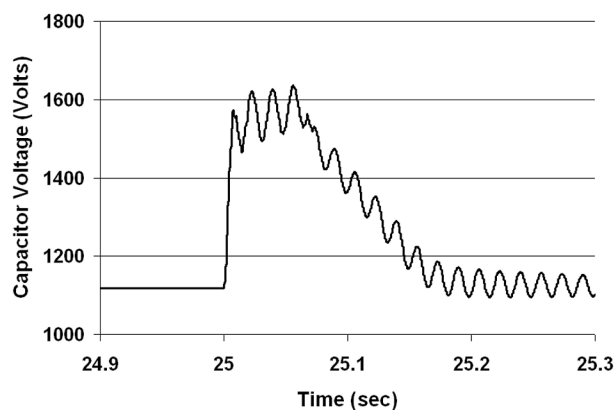


Fig. 8. 4-cycle 1 mohm Fault at Generator Terminals – DC Capacitor Voltage - Detailed Model.

Shown in Fig. 8 is such a rise in capacitor voltage as simulated by the detailed model for the test fault. There is no

"stability model" counterpart of this figure, because such dynamics was assumed instantaneous in the stability model.

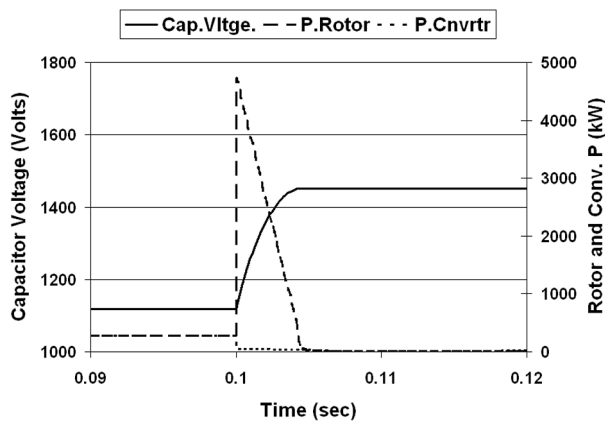


Fig. 9. 4-cycle 1 mohm Fault at Generator Terminals – Estimation of DC Capacitor Voltage from Stability Model results.

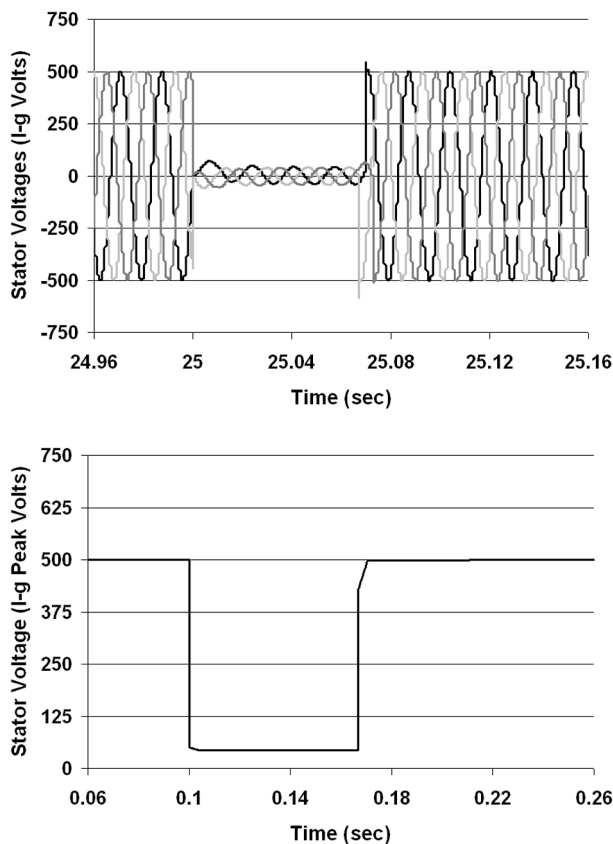


Fig. 10. 4-cycle 1 mohm Fault at Generator Terminals – Stator Voltages - Detailed vs. Stability Models (3-phase components for Detailed Model, peak positive sequence component for Stability Model).

An approximate estimate of the capacitor voltage rise is however possible by integration of the discrepancy between rotor and converter-side active powers, (as approximated by the stability model) as energy stored in the capacitor; thus deriving the capacitor voltage (Fig. 9). Although imprecise (a rise to 1450V, 180V lower than the maximum voltage indicated by the detailed model), such calculations could be

used as a first screening of contingency scenarios that require detailed analysis. Of course, the precision of these calculations could be improved by extending the modeling to the stator-side converter controls, as well as modeling capacitor dynamics. However, detailed studies of DFIG performance during faults would still need the more detailed EMT-type models; particularly if, as it is likely the case, performance following unbalanced faults is of interest.

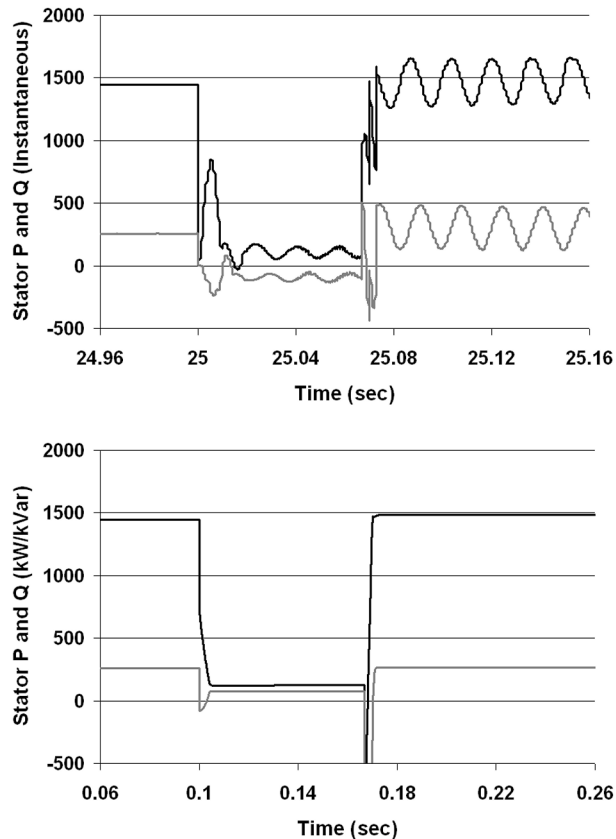


Fig. 11. 4-cycle 1 mohm Fault at Generator Terminals – Stator Active and Reactive Powers - Detailed vs. Stability Models.

Note that, since PWM switching effects are neglected in the detailed model, the voltage surge shown in Figure 8 is slightly higher than would be shown in a comparable simulation with full representation of the PWM switching system. PWM switching gives a slight damping effect that is not included in the detailed model, and thus the detailed model gives conservative conditions with respect to capacitor voltage rise during the fault.

Finally, Figs. 10 and 11 compare detailed and stability model stator terminal voltages and active and reactive powers, respectively. If the effect of dc components is discounted in the detailed model results, an excellent agreement is observed, thus completing the large-signal validation of the transient stability model.

V. CONCLUSIONS

This paper presents and validates a model for DFIG wind units suitable for transient stability studies. The approach used was the representation of some of the main aspects of DFIG, without compromising its applicability for large simulation studies. The results suggest that the model has sufficient accuracy for representation of the electromechanical dynamics of interest in transient stability studies.

The model also includes representation of generator flux dynamics and of the dynamics of rotor-side current controllers. In DFIG those effects are too fast to have an impact on electromechanical dynamics. They are critical, however, in the assessment of whether or not the wind generation will trip following a disturbance, and thus have a significant bearing on simulation results.

Thus, the transient stability model can be used as a screening tool in identifying critical contingency scenarios and/or in establishing minimum requirements for "ride-through" capability of voltage-source converters. This is a very important parameter to be included in the specification and in discussions with wind turbine/generator manufacturers. Further analysis of these critical conditions may require the use of more detailed EMTP (or EMTDC, or Matlab/Simulink) - level models, with accurate representation of the impact of non-linearities, dc-components, and unbalanced operation; among other effects.

REFERENCES

- [1] R. Pena, J. C. Clare, G.M. Asher, "Doubly fed induction generator using back-to-back PWM converters and its application to variable-speed wind-energy conversion", IEE Proceedings-Electric Power Applications, v.143,n.3, May 1996, pp.231-241.
- [2] R.J. Koessler, "Dynamic Simulation of Static Var Compensators in Distribution Systems," IEEE Transactions on Power Systems, Vol. 7, No. 3, August 1992.
- [3] *PSS/E Program Application Guide, Volume II*, Power Technologies Inc., Schenectady NY 2001.
- [4] P. Pourbeik, R.J. Koessler, D.L. Dickmader, and W. Wong, "Integration of Large Wind Farms into Utility Grids (Part 2 – Performance Issues)", submitted for presentation at IEEE PES General Meeting 2003.

Rodolfo J. Koessler (M'84, SM'93) received an M.E. degree in Power Systems from the Rensselaer Polytechnic Institute, Troy, NY in 1982. From 1985 to 2000 he was with Power Technologies, Inc., where most of his work was in the areas of dynamic performance and model development. He joined ABB in 2000 as an Executive Consultant with the Consulting Division. Mr. Koessler has authored/coauthored over 30 technical papers and articles.

Srinivas Pillutla (M'98) received his Ph.D degree in electrical engineering from the Ohio State University, Columbus, OH, in 1999. From 1998 to 2000, he worked at Power Technologies, Inc. in Schenectady, NY. Since 2001, he has been working with ABB Inc. as a Consulting Engineer. His research interests are in generator and power system equipment modeling.

Lan H. Trinh (M'00) received his M.S. and Ph.D. degrees from Moscow Power Institute, Moscow, Russia, in 1990 and 1993 respectively. Since 1997 he has been employed by ABB. His interests include power system modeling, power system control and wind power.

David L. Dickmader (M'84) received his MS degree in electrical engineering from Purdue University in 1984. In 1984, he joined ABB and since then he has worked at ABB locations in Sweden and the U.S., most recently Raleigh, NC. His work at ABB has covered analytical studies for a broad range of power electronics systems, including HVDC, SVC, TCSC, STS, and TSR systems. He has also been responsible for detailed control design and DSP software development for medium voltage products and converters for fuel cell and photovoltaics applications. Mr. Dickmader is a member of Tau Beta Pi, Eta Kappa Nu, and IEEE. He has authored IEEE papers in the areas of harmonics, harmonic interactions, and TCSC and SVC controls.